Electronic Supplementary Material (ESI) for Journal of Materials Chemistry A.

Comprehensive Interface Engineering Based on Target Anchoring Agents towards Efficient and Stable Inverted Perovskite Solar Cells

Authors: Pengpeng Dong[1], Bitao Chen[1], Disheng Yao[*1,2], Songbo Li[1], Jiale Su[1], Bing Zhou[1], Nan Tian[1], Guoyuan Zheng [1,2], Yong Peng[3], Fei Long[*1,2]

1 Guangxi Key Laboratory of Optical and Electronic Material and Devices, School of Materials Science and Engineering, Guilin University of Technology. 12 Jiangan Road, Guilin, Guangxi 541004, China

2 Collaborative Innovation Center for Exploration of Nonferrous Metal Deposits and Efficient Utilization of Resources, Guilin University of Technology. 12 Jiangan Road, Guilin, Guangxi 541004, China

3 State Key Lab of Advanced Technology for Materials Synthesis and Processing, Wuhan University of Technology, Wuhan, Hubei 430070, China

E-mail: yaodisheng@glut.edu.cn (Disheng Yao), longf@glut.edu.cn (Fei Long)

Experimental Section

Materials

Cesium iodide (CsI), formamidinium iodide (FAI), lead bromide ($PbBr_2$), methylammonium chloride (MACl), methylammonium bromide (MABr), PCBM were purchased from Advanced Election Technology in China. Lead iodide (PbI_2), 4,4',4''-tri(N-phenyl-N-m-tolyl-amino)triphenylamine (m-MTDATA), phenyl ammonium bromide (PhABr), poly[[bis(4-phenyl)(2,4,6-trimethylphenyl)amine]] (PTAA) (Mn 6000-15000), and bathocuproine (BCP, purity 99.9%) were purchased from Xi'an Polymer Light Technology Corporation. The solvents, including dimethylformamide (DMF), dimethyl sulfoxide (DMSO), isopropanol (IPA), and chlorobenzene (CB) were purchased from Advanced Election Technology in China. Glass substrates patterned with indium tin oxide (ITO) (15 Ω sq^{-1}) were custom-patterned in our laboratory.

Substrate preparation

The glass/ITO substrates underwent a sequential ultrasonic cleaning process for 20 minutes involving detergent, deionized water, acetone, and alcohol. Subsequently, these glass/ITO substrates were dried in an oven at 60 °C. Afterward, they were exposed to a 15-minute-long treatment with 100 mW ozone plasma and then transferred into a glovebox filled with nitrogen (N_2), where the contents of oxygen (O_2)/water (H_2O) maintained at <10/0.01 ppm.

Preparation of PTAA and PTAA/m-MTDATA HTLs

A precursor solution for the hole transport layer (HTL), with a thickness of <20 nm, was prepared by dissolving PTAA in toluene at a concentration of 2 mg/ml. This solution was spin-coated onto the ITO substrate at 4000 rpm for 30 s, followed by annealing at 100 °C for 10 min. An intermediate layer of PTAA/Perovskite was preparedby dissolving m-MTDATA in DMF at varying concentrations. It was then spin-coated onto the ITO substrate at 6000 rpm for 30 s and annealed at 100 °C for 3 min.

Fabrication of perovskite films

A perovskite precursor solution was prepared by mixing CsI, FAI, MABr, PbI_2, and $PbBr_2$ in 1 mL of DMF: DMSO (5:1 / v:v) mixed solvent. The chemical formula for the perovskite precursor solution was $Cs_{0.07}MA_{0.02}FA_{0.91}PbI_{2.94}Br_{0.06}$, resulting in a perovskite precursor solution with a total molar quantity of 1.73 M. In order to promote the growth of perovskite crystal grains, we increased the PbI_2 content by 5 mol.%. After stirring at room temperature for 1 h, 5 mol.% of MACl was added, followed by an additional 1-hour stirring at 60 °C. Hundred microliters perovskite solution were spin-coated onto the glass/ITO/HTL at 1000 rpm for 10 s, followed by a spin-coating step at 5000 rpm for 35 s. In the second step, 200 μL of CB was dispensed onto the film's center at a rate of 25 s with a distance of 1 cm. The resultant perovskite film was annealed at 100 °C for 30 min.

"Chemical polishing" with PhABr

A PhABr precursor solution was created by dissolving 37.5 mg PhABr in 1 mL of IPA. The follow-up "chemical polishing" solution was prepared by extracting 40 μL of the precursor solution and dissolving it in 1 mL CB. This solution was stirred for 10 min before being spin-coated onto the perovskite substrate at 5000 rpm for 30 s.

Subsequently, to strengthen the polishing effect, 100 μL CB was poured onto the perovskite film, and another 100 μL CB was then spin-coated onto the perovskite film. The repeated wash with CB removed residual PhABr and reaction products of PhABr and PbI_2.

Preparation of electron transport layer and electrode

The precursor solution of the ETL was prepared by dissolving PCBM with a concentration of 20 mg / mL in CB. The ETL solution was spin coated on the perovskite film at 1600 rpm for 30 s. Afterward, the 150 μL of BCP saturated solution was spin coated on the ETL at 5000 rpm for 17 s. Finally, 100 nm silver electrode was thermally evaporated at a rate of 1.0 A s^{-1} under high vacuum ($<4 \times 10^{-5}$ Torr). The active area of the device was 0.058 cm^2.

Characterization

Ultraviolet Photoelectron Spectroscopy (UPS) and X-ray Photoelectron Spectroscopy (XPS) measurements were conducted using an ESCALAB 250Xi and Thermo Fisher (Al Kα X-ray source). In all XPS measurements, the characteristic peak of C 1s was calibrated to 284.8 eV. Ultraviolet/Visible (UV-Vis) spectra were obtained using a Shimadzu 3600 UV-Vis spectrophotometer. Scanning electron microscope (SEM) images were acquired using an S4800 field-emission scanning electron microscope. Electrochemical impedance spectroscopy (EIS) measurements were carried out under dark conditions using a ZENNIUM electrochemical workstation from Zahner, Germany. X-ray diffraction (XRD) patterns of different samples were obtained using a PANalytical b.v. X Pert PRO X-ray diffractometer. UV/Visible/Near-infrared diffuse reflectance measurements were performed using a Shimadzu UV-3600i Plus spectrophotometer. Contact angle tests were conducted on a Kenor SL200B/K contact angle analyzer from the USA. Steady-state photoluminescence (PL) spectra were measured using a Horiba Quanta Master 8000. Time-Resolved Photoluminescence (TR-PL) measurements were carried out using the FLS1000 system from Edinburgh Instruments Limited, with an excitation wavelength of 485 nm. Atomic Force Microscopy (AFM) and Kelvin Probe Force Microscopy (KPFM) images were obtained using a Bruker Dimension Icon atomic force microscope in contact mode. Conductive Atomic Force Microscopy (C-AFM) measurements were performed with a Bruker Nanowizard 4XP atomic force microscope using an SCM-PIT-v2 probe for C-AFM detection.

Theoretical calculation of Density functional theory (DFT)

Our spin-polarized density functional theory (DFT) calculations[1,2] were carried out in the Vienna ab initio simulation package (VASP) based on the plane-wave basis sets with the projector augmented-wave method[3,4]. The exchange-correlation potential was treated by using a generalized gradient approximation (GGA) with the Perdew-Burke-Ernzerhof (PBE) parametrization[5]. The van der Waals correction of Grimme's DFT-D3 model was also adopted[6-7]. The supercell of $FAPbI_3(001)$ surface was constructed and the C_6H_8BrN (PhABr) adsorbed on it. The energy cutoff was set to be 400 eV. The Brillouin-zone integration was sampled with a Γ-centered Monkhorst-Pack mesh of 1 × 1 × 1, and the 2 × 2 × 2 k-points was used to calculate single point energy. The convergence threshold of energy in the self-consistent step was set as 10^{-5} eV with

Gaussian smearing of 0.01 eV/Å, and the force threshold of geometry optimization is 0.02 eV/Å for each dimension of all atoms in supercell. The adsorption energy, E_{ads} was computed using the following equation:

$$E_{ads} = E_{complex} - [E_{slab} + E_{adsorbates}].$$

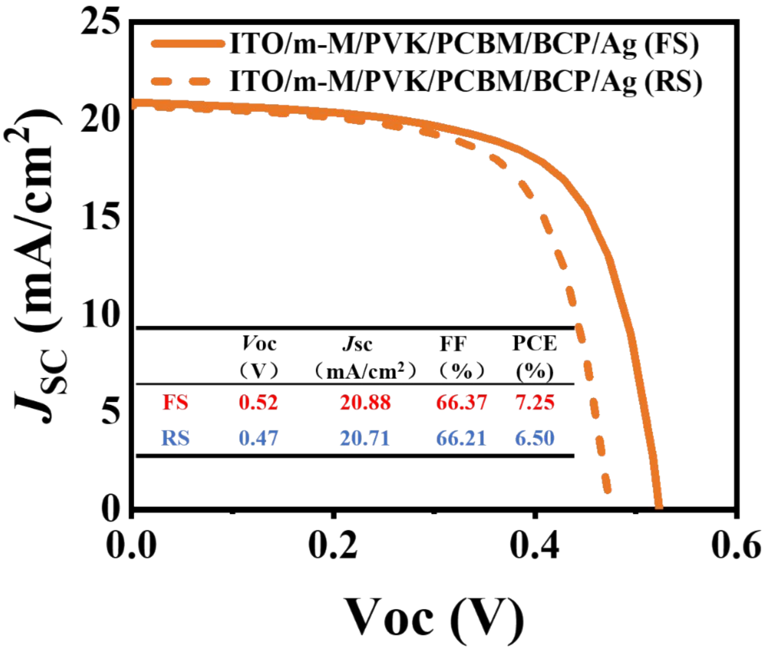

	*V*oc（V）	*J*sc（mA/cm^2）	FF（%）	PCE (%)
FS	0.52	20.88	66.37	7.25
RS	0.47	20.71	66.21	6.50

Figure S1. I-V characteristics of devices with m-MTDATA as HTL at a concentration of 2 mg/ml in toluene. The table in the figure shows the data of each test.

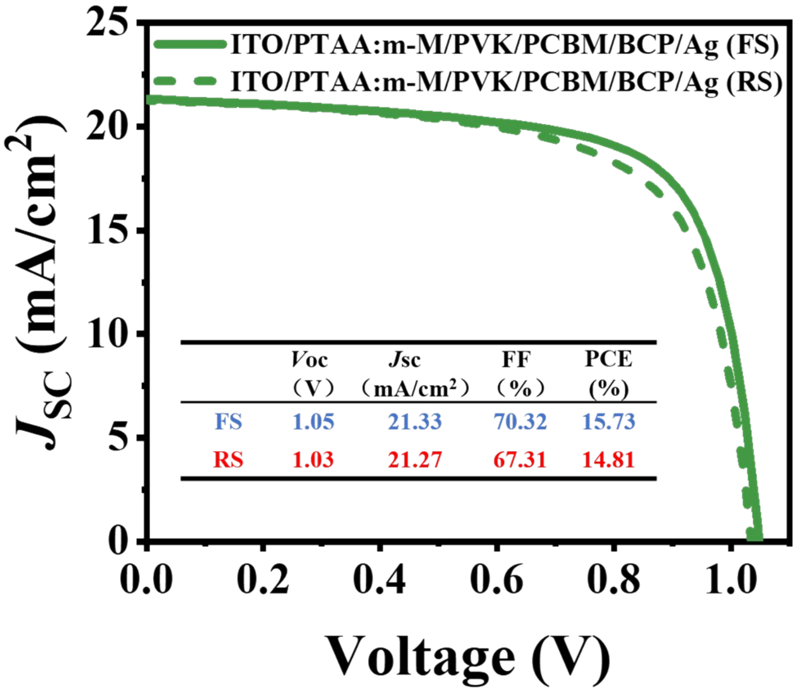

	*V*oc（V）	*J*sc（mA/cm^2）	FF（%）	PCE (%)
FS	1.05	21.33	70.32	15.73
RS	1.03	21.27	67.31	14.81

Figure S2. I-V characteristics of devices with m-MTDATA as dopant of PTAA at a concentration of 0.5 mg/ml in PTAA. The table in the figure shows the data of each test.

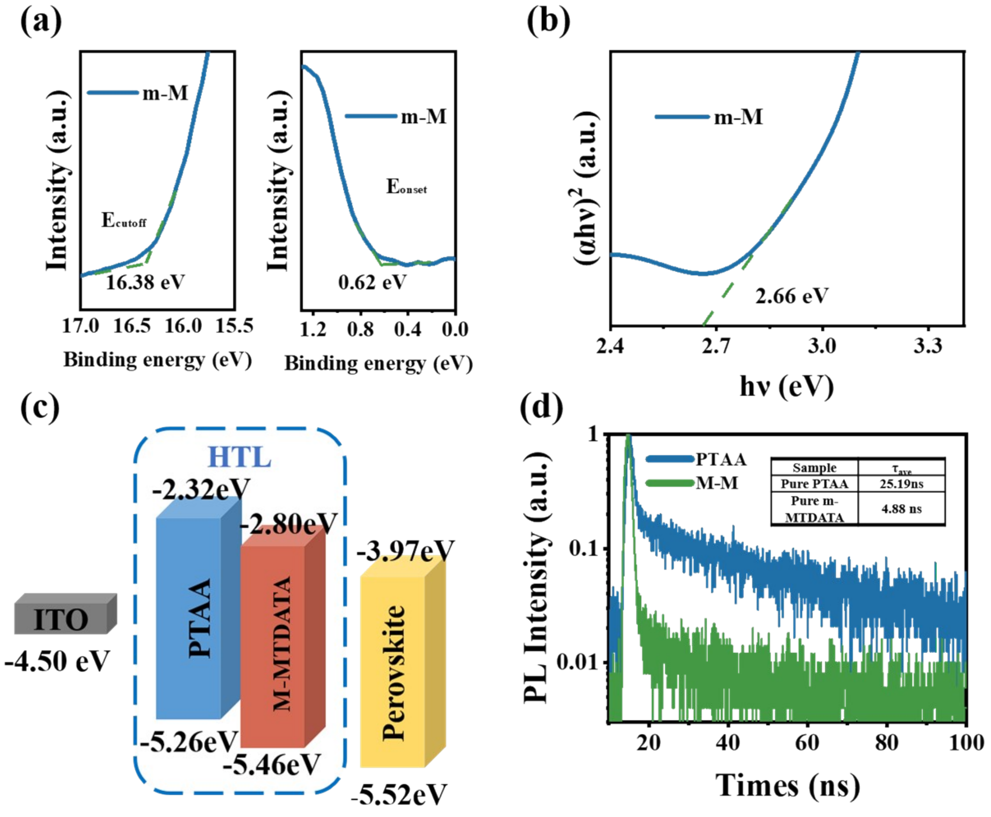

Sample	τ_{ave}
Pure PTAA	25.19ns
Pure m-MTDATA	4.88 ns

Figure S3. **a)** UPS of m-MTDATA. **b)** UV-Vis spectrum of m-MTDATA. **c)** Energy level diagram of the PTAA and m-MTDATA. **d)** TR-PL curves of the pure PTAA and m-MTDATA device structure

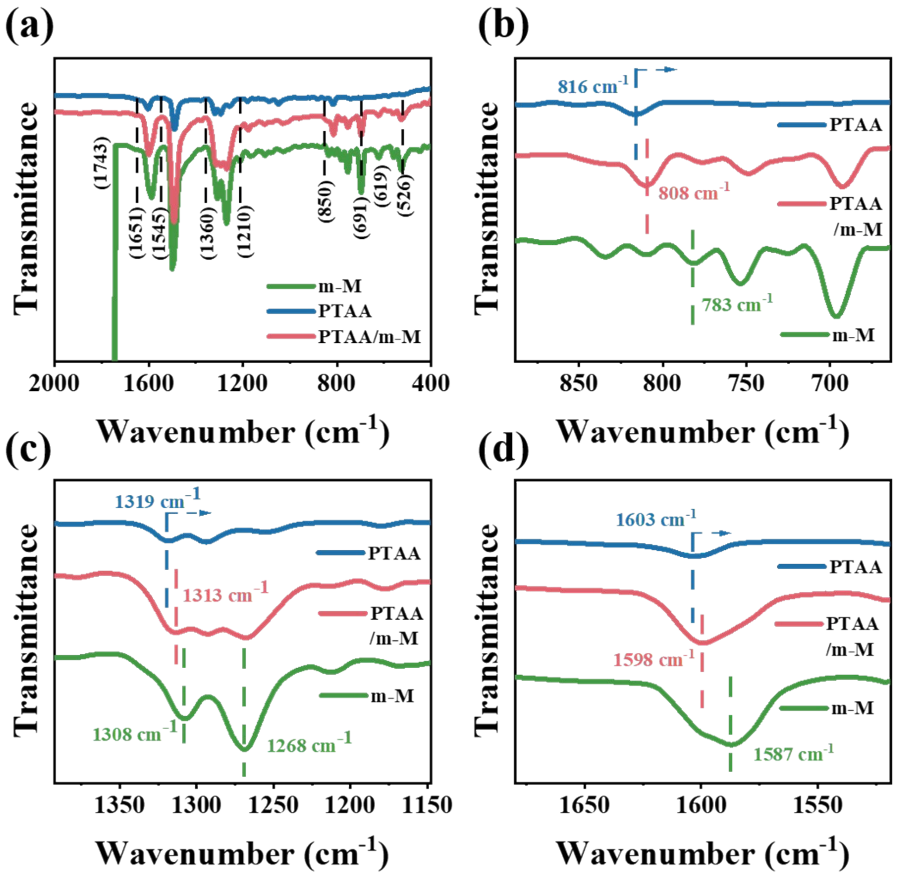

Figure S4. **a)** FTIR spectra of PTAA, m-MTDATA and PTAA/m-M Locally amplified FTIR spectra of PTAA, m-MTDATA and PTAA / m-M: **b)** bands of 690 cm^{-1} - 850 cm^{-1} **c)** bands of 1210 cm^{-1} - 1360 cm^{-1} **d)** bands of 1545 cm^{-1} - 1651 cm^{-1}.

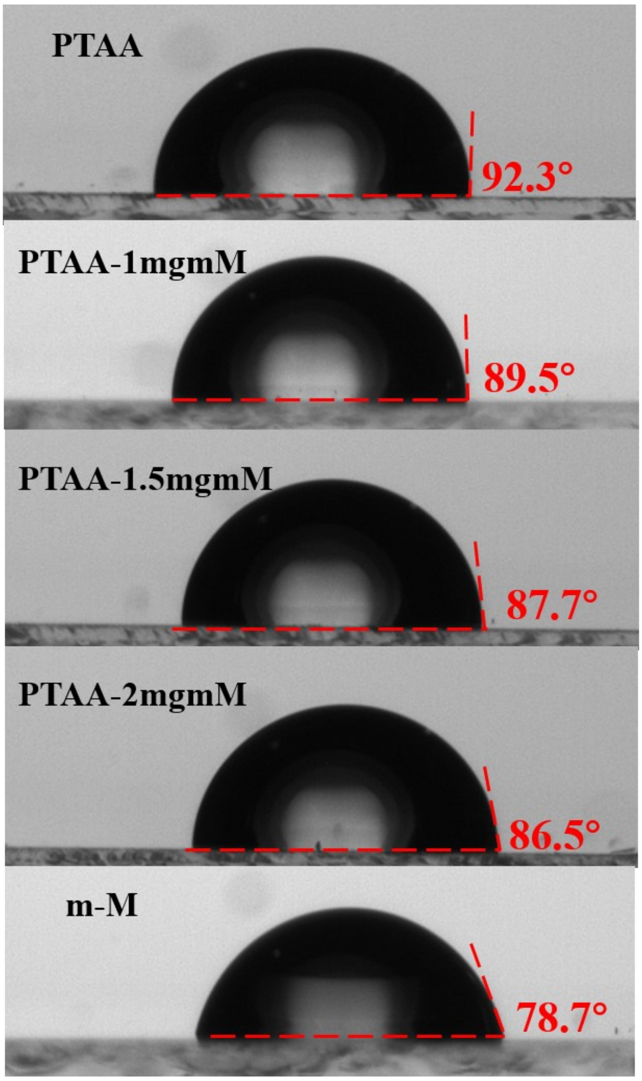

Figure S5. Contact angle measurements of PTAA, m-MTDATA-modified PTAA, and m-MTDATA thin films with DMF. Droplet volume: 5 μL

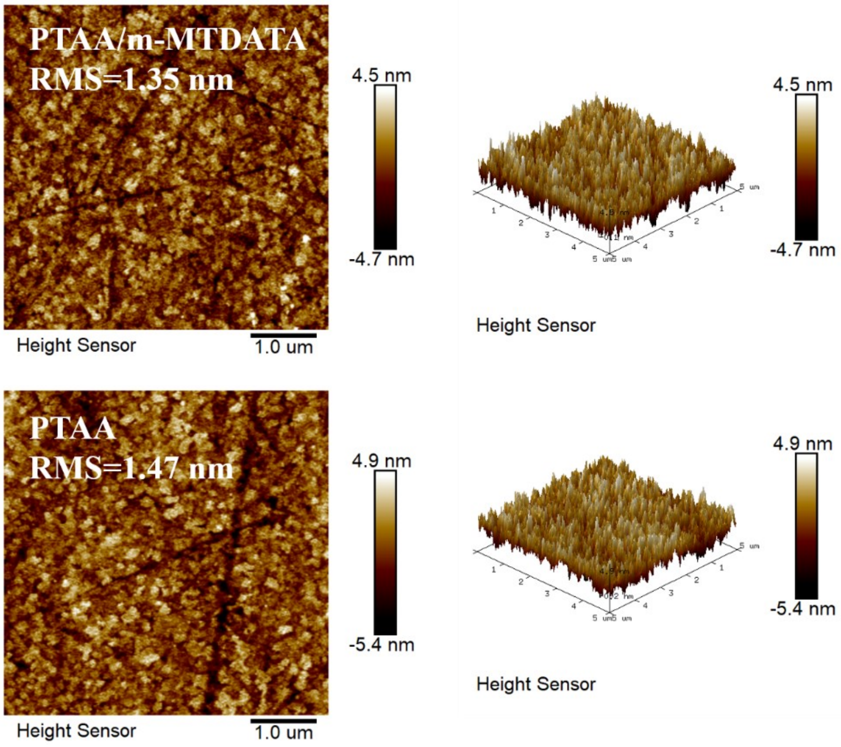

Figure S6. Surface characterization of PTAA-based and m-MTDATA-modified PTAA films using atomic force microscopy (AFM).

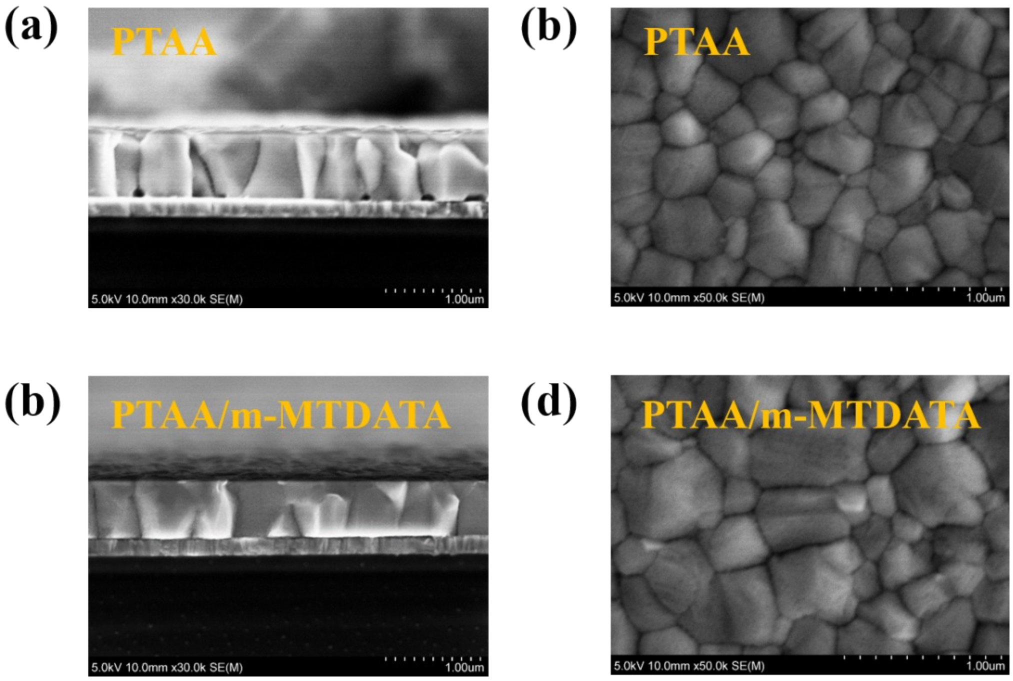

Figure S7. Top-View and Cross-Sectional SEM images of PVK-coated films on PTAA and m-MTDATA-modified PTAA. **a)** Cross-sectional image of PTAA/PVK. **b)** Cross-sectional image of PTAA/m-MTDATA/PVK. **c)** Top-view image of PTAA/PVK. **d)** Top-view image of PTAA/m-MTDATA/PVK

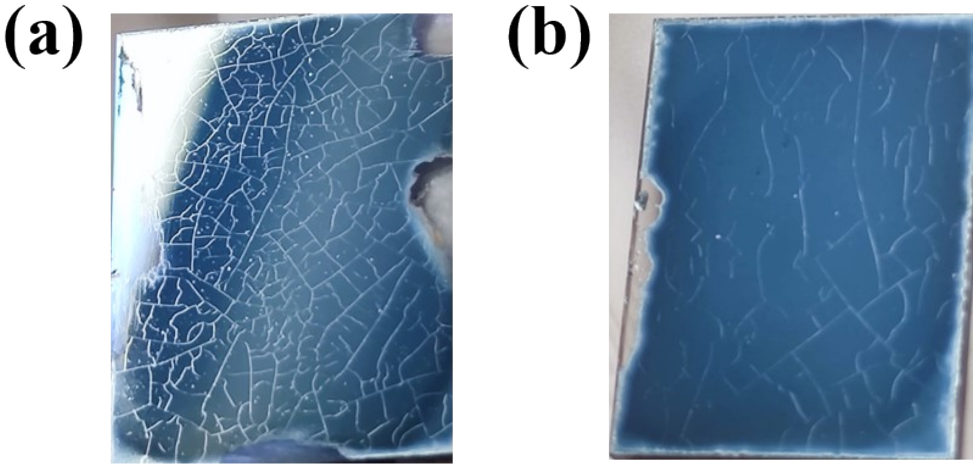

Figure S8. a) Photograph of spin-coated perovskite film on PTAA. **b)** Photograph of spin-coated perovskite film on PTAA/m-MTDATA.

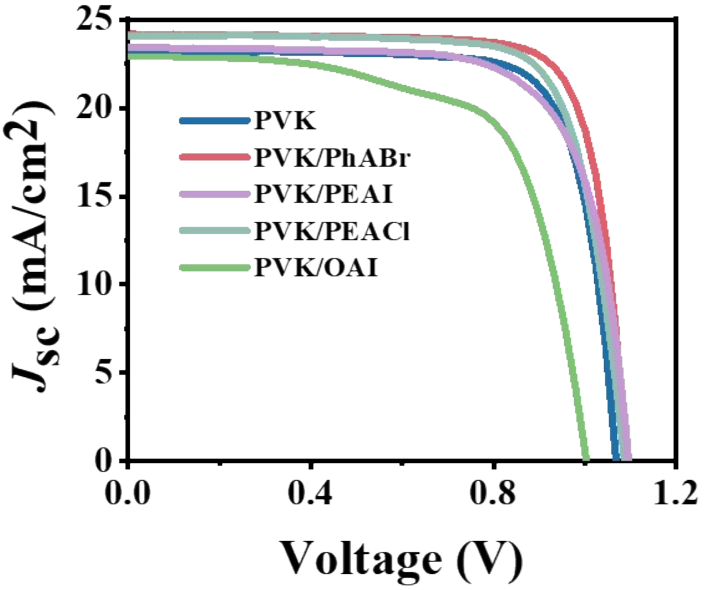

Figure S9. I-V characteristics of devices with Perovskite, Perovskite/PhABr, Perovskite/PEACl and Perovskite/OAI.

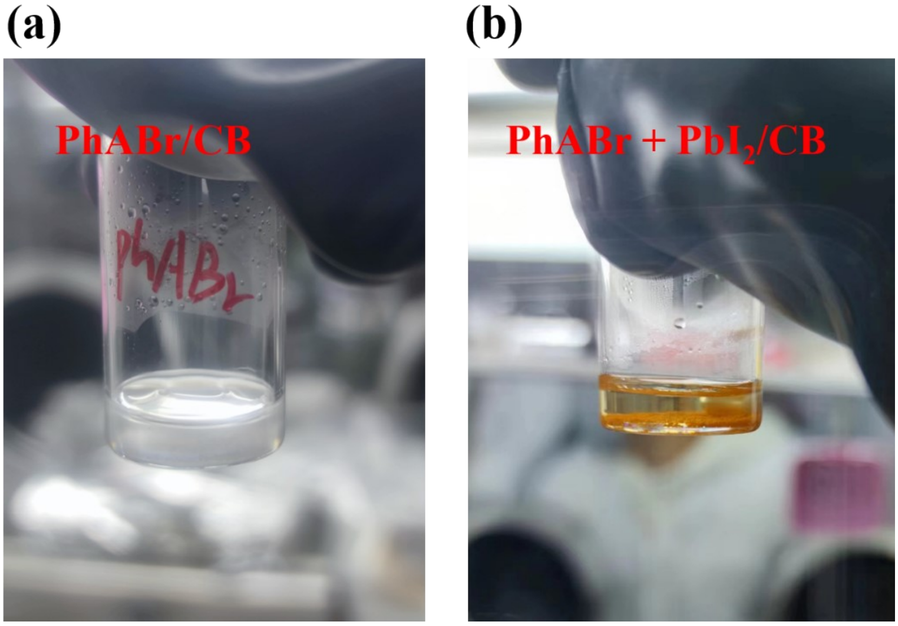

Figure S10. **a)** Photograph of PhABr solution. **b)** Photograph of PhABr + PbI_2 solution.

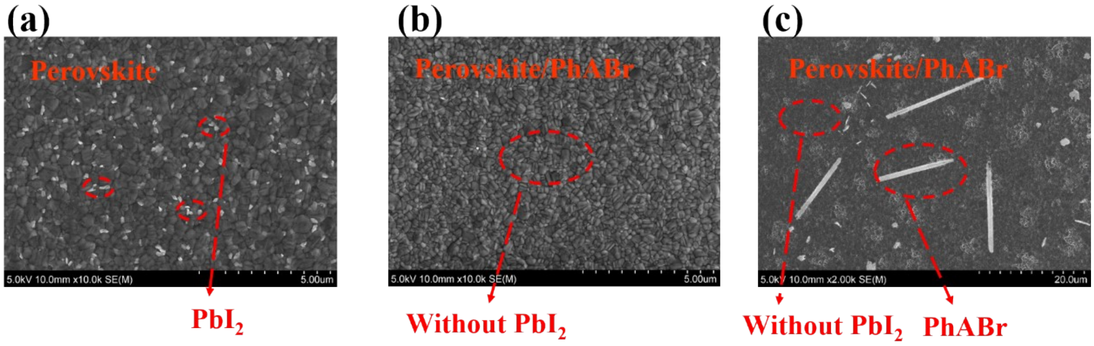

Figure S11. **a)** Top-View images of Perovskite **b)** Top-View images of Perovskite/PhABr **c)** SEM picture of drug residue on the surface of PhABr treated perovskite

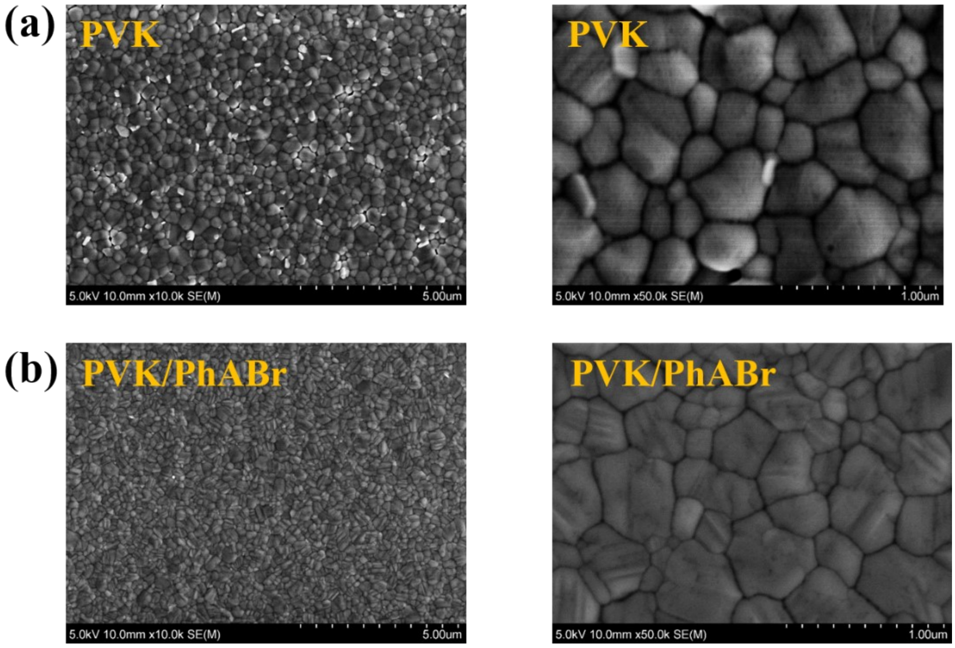

Figure S12. Top-View images of PhABr spin-coated on PVK films. **a)** Top-view images of PVK 10 k and 50 k. **b)** Top-view images of PVK/PhABr 10 k and 50 k.

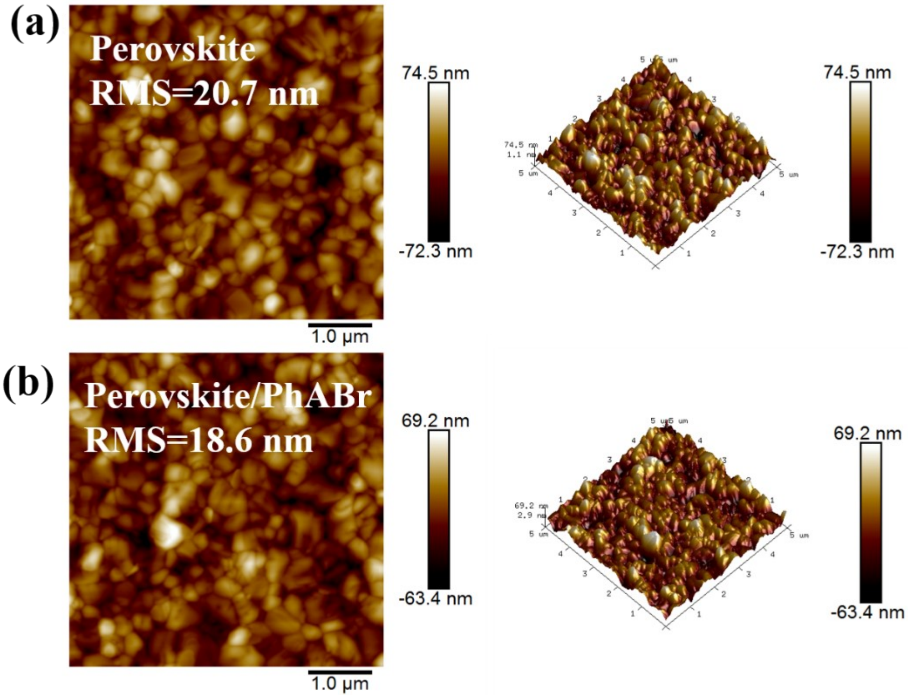

Figure S13. Surface characterization of PVK-based **a)** PhABr-modified PVK films **b)** using btomic force microscopy (AFM).

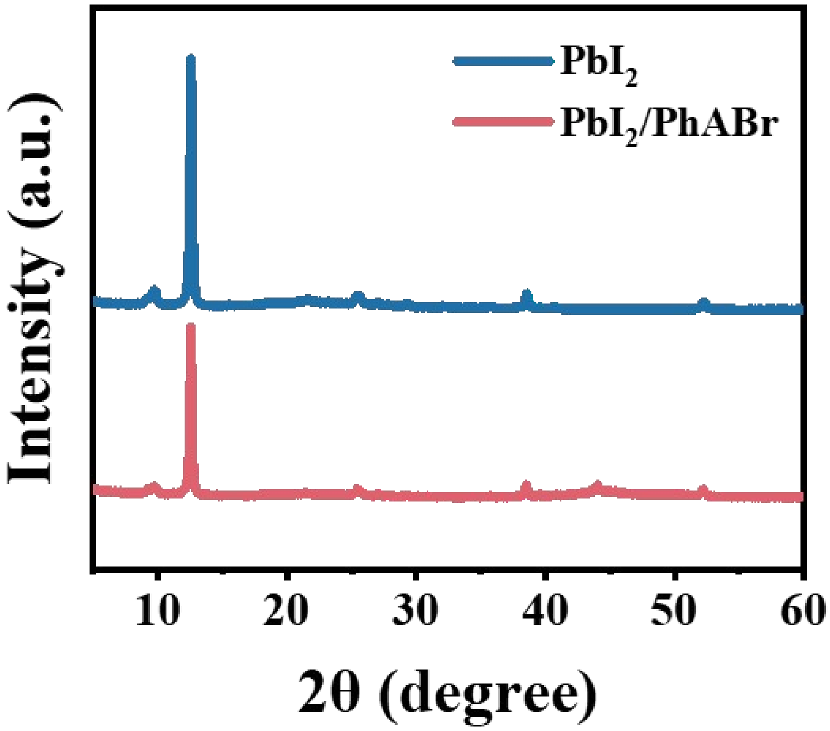

Figure S14. XRD comparison of the phase of PbI_2 deposited on quartz glass before and after treatment with PhABr.

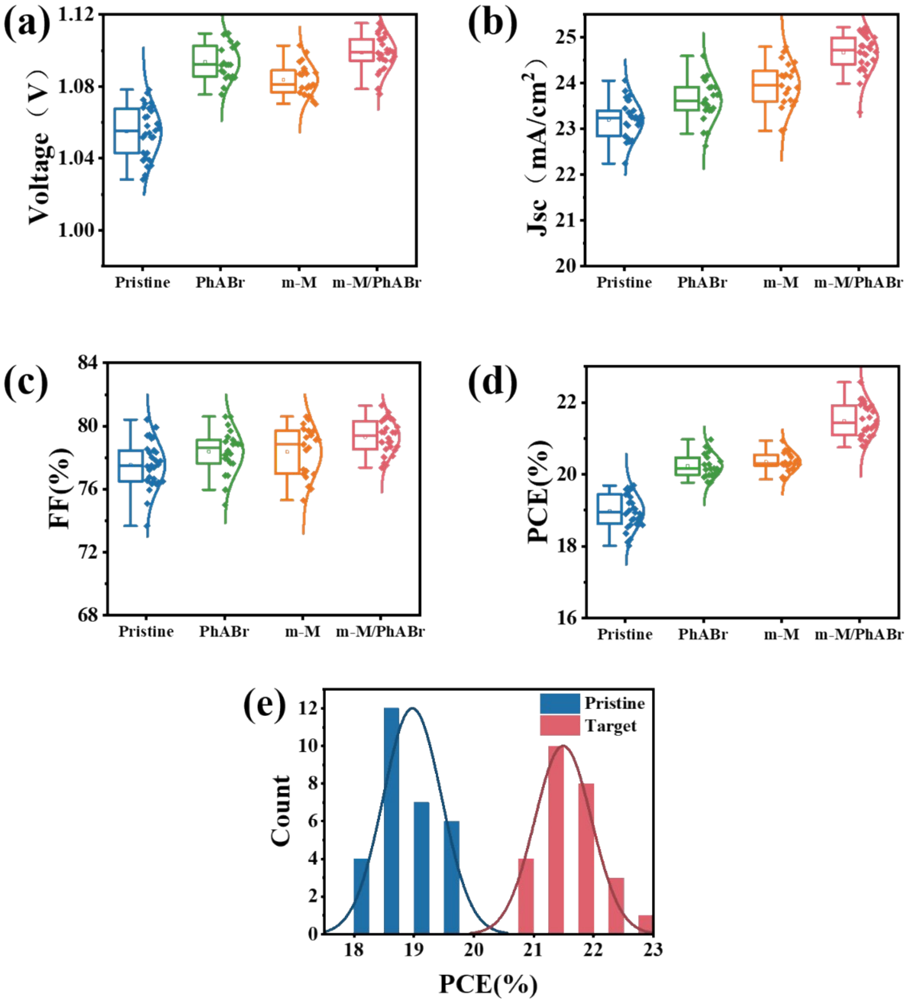

Figure S15. Performance metrics of original and targeted perovskite solar cells (PSCs): **a)** Open circuit voltage (V_{OC}). **b)** Short circuit current density (J_{SC}). **c)** fill factor (FF). **d)** Power conversion efficiency (PCE) statistics. **e)** Histogram of PCEs for control and targeted devices

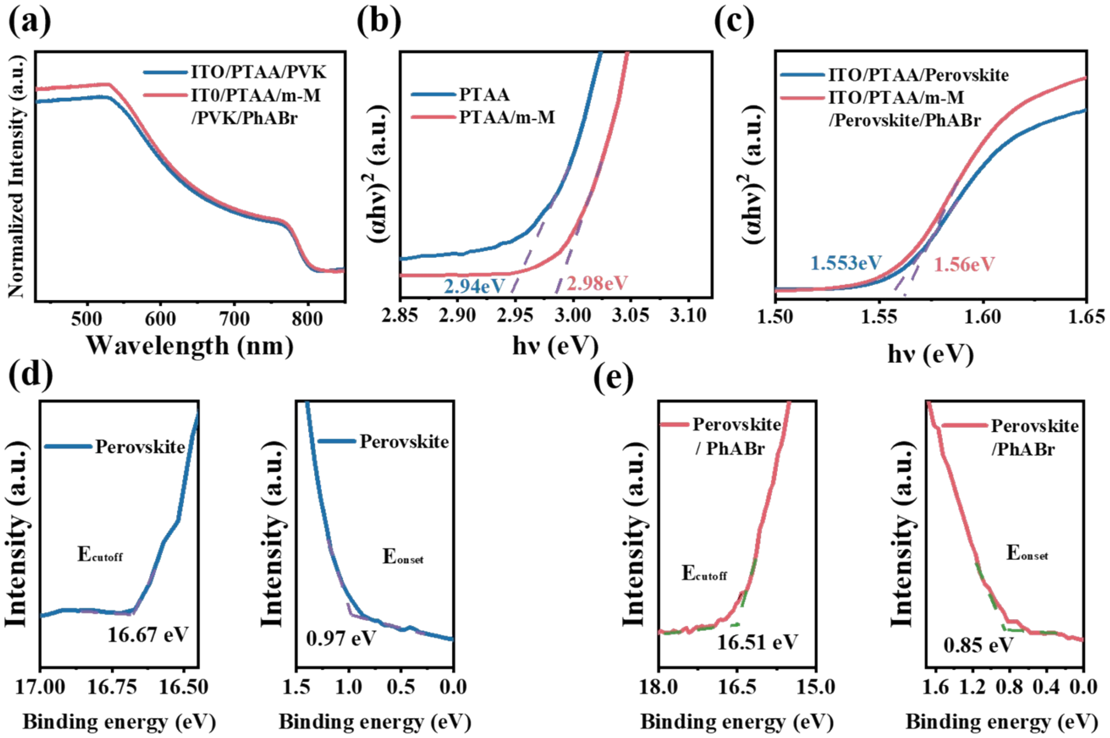

Figure S16. **a)** UV-Vis absorption spectra of the pristine and target devices. **b)** UV-Vis spectra of PTAA and m-MTDATA-modified PTAA thin films. **c)** UV-Vis spectra of original Perovskite and Perovskite modified by m-M and PhABr.. **d)** UPS of Perovskite. **e)** UPS of Perovskite/PhABr.

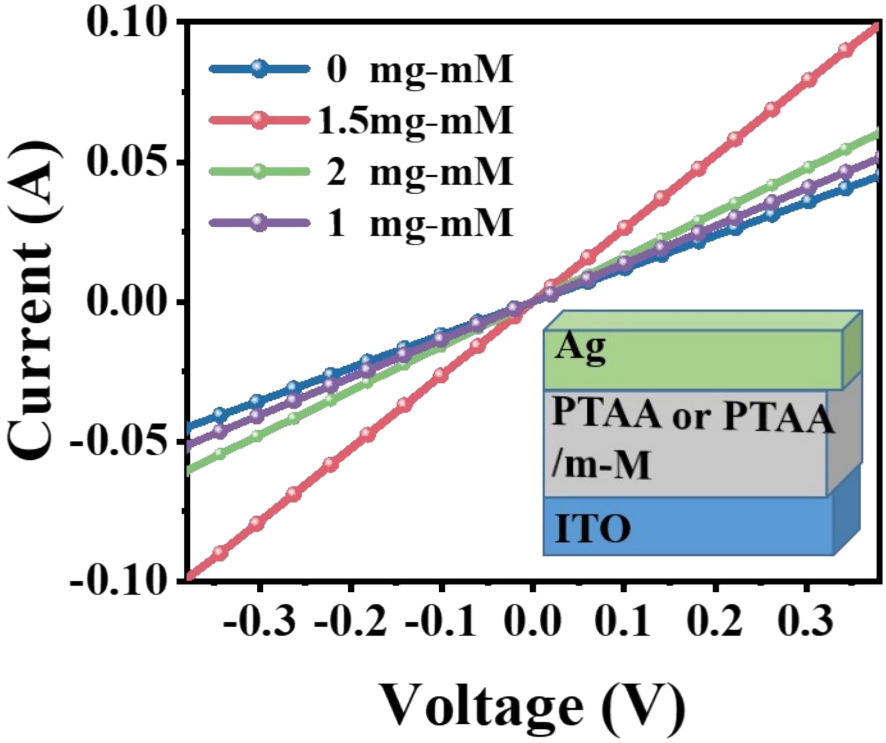

Figure S17. Conductivity curves of PTAA and m-MTDATA-modified PTAA at various concentrations. Inset: structural of samples taking the structure of ITO/PTAA(PTAA-mMTDATA)/Ag.

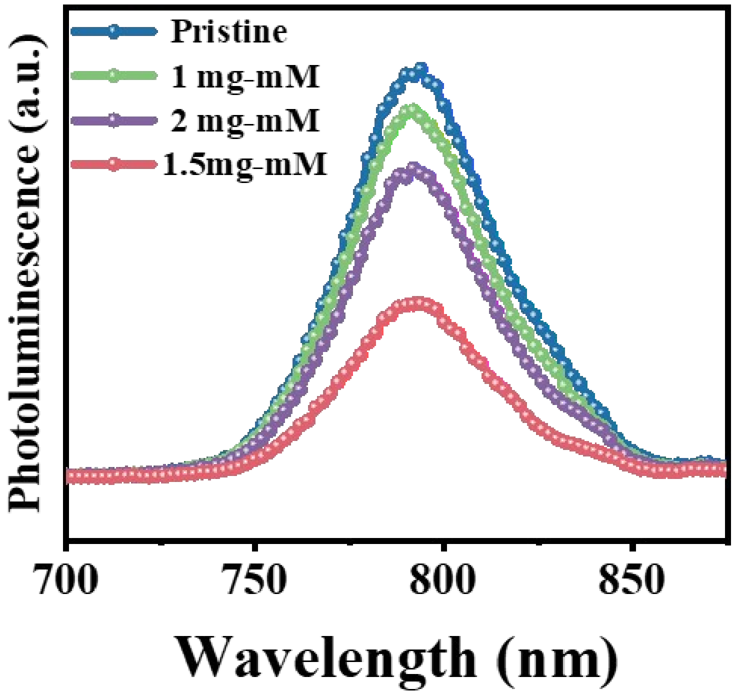

Figure S18. Photoluminescence (PL) curves of devices with different concentrations of m-MTDATA modification.

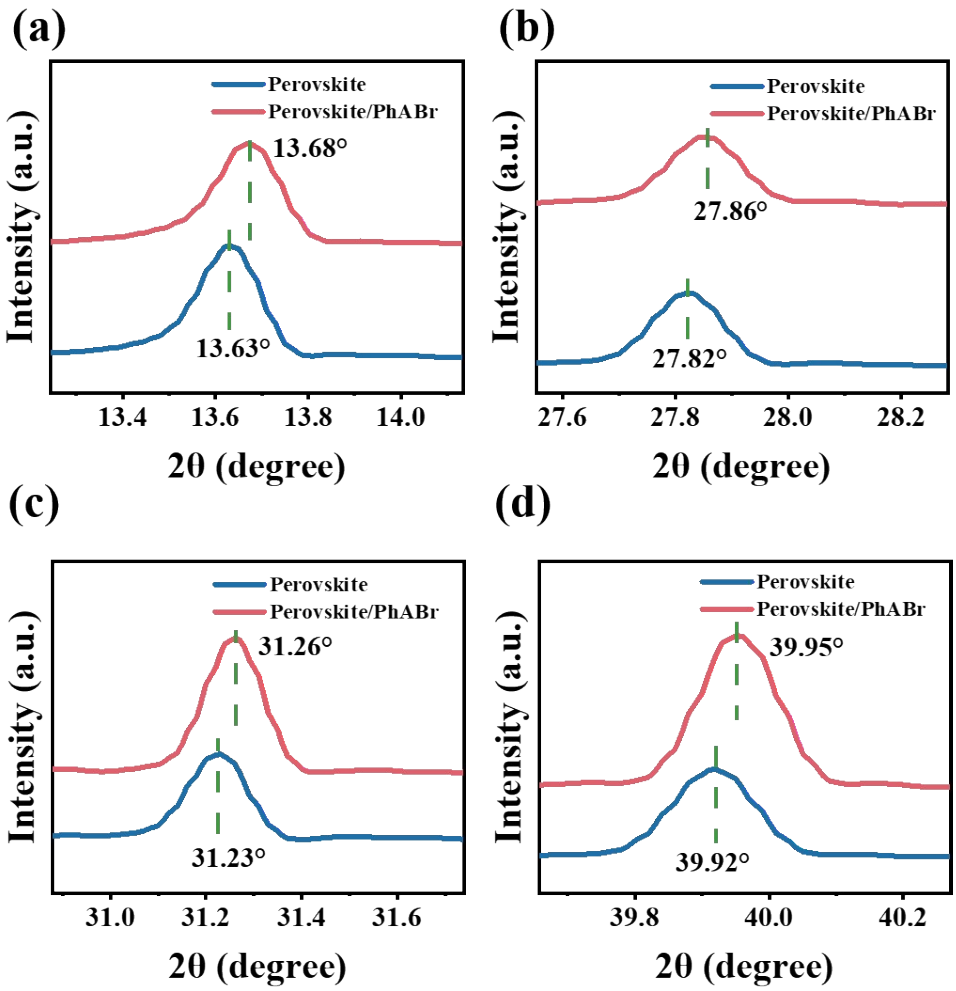

Figure S19. The enlarged crystal faces of perovskite **a)** (110), **b)** (220), **c)** (310) and **d)** (224).

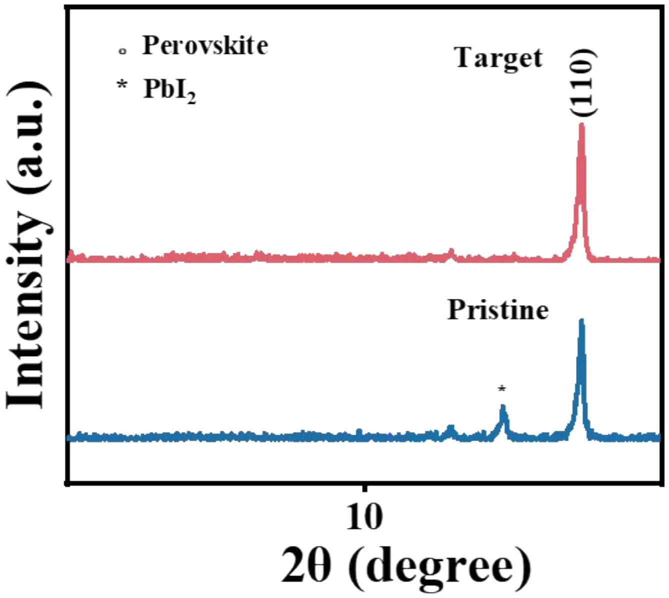

Figure S20. The enlarged crystal faces of perovskite from 5° to 15° at 2θ

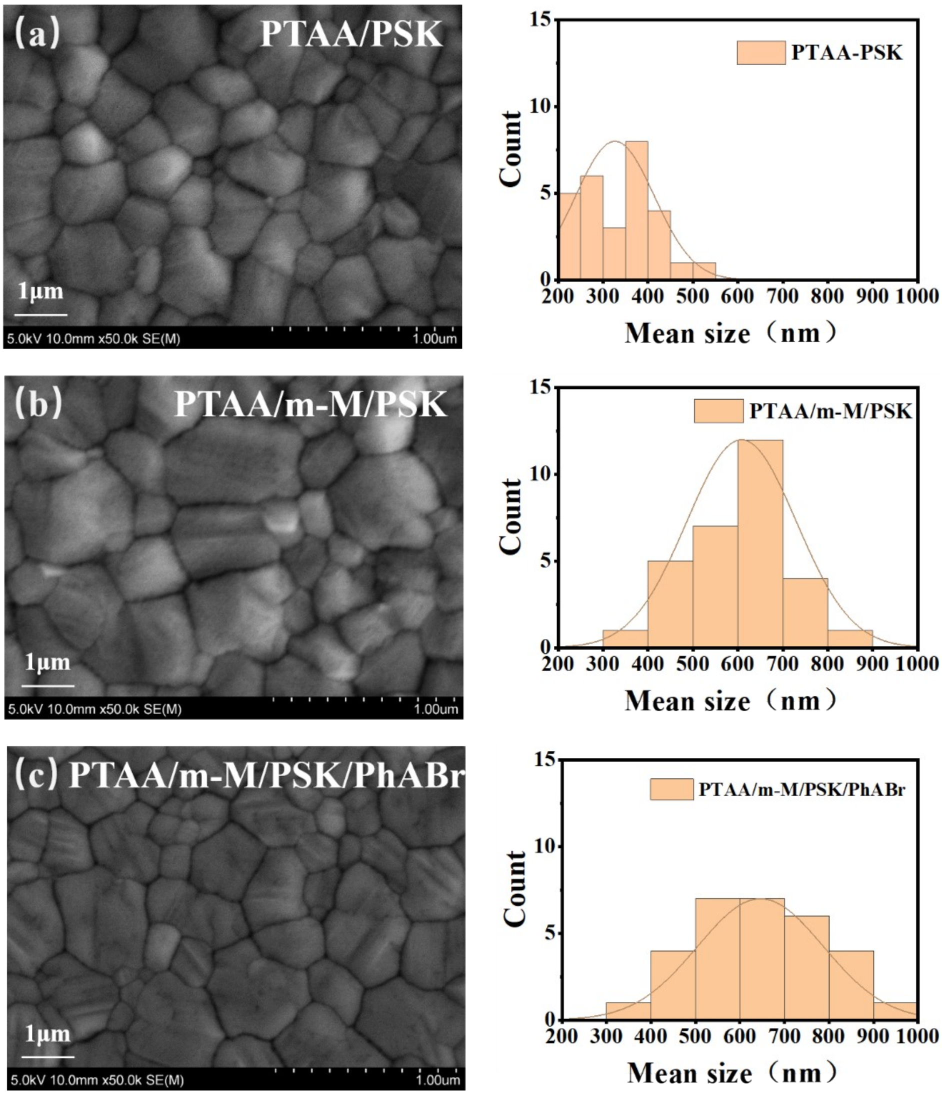

Figure S21. Top-View SEM images and particle size histograms of PVK films coated on: **a)** PTAA. **b)** m-MTDATA-modified PTAA. **c)** Dual-Layer modified PVK surfaces.

Table S1: TRPL curve fitting parameters of perovskite on original devices.

Sample	A_1	$\tau_{1\ (ns)}$	A_2	$\tau_{2\ (ns)}$	$\tau_{ave\ (ns)}$
PTAA	222.56	0.93	35.29	30.00	25.19
m-M	598.97	0.63	5.59	19.56	4.88

Table S2. Detailed photovoltaic parameters of Perovskite, Perovskite/PhABr, Perovskite/PEACl and Perovskite/OAI.

	V_{oc} (V)	J_{sc} (mA/cm^2)	FF (%)	PCE (%)
PVK	1.068	23.25	76.94	19.12
PVK/PhABr	1.091	24.15	78.97	20.80
PVK/PEAI	1.096	23.42	72.09	18.50
PVK/PEACl	1.087	24.05	76.12	19.90
PVK/OAI	1.003	22.94	66.61	15.34

Table S3. Detailed photovoltaic parameters of PSCs fabricated with Perovskite thin films as shown in the table.

		V_{OC} (V)	J_{SC} (mA/cm^2)	FF (%)	PCE (%)
Pristine	Forward	1.063	23.74	78.01	19.69
	Reverse	1.054	23,53	75.97	18.84
Target	Forward	1.115	25.16	80.42	22.56
	Reverse	1.107	25.12	79.23	22.04

Table S4. Performance parameters of PSCs prepared by spin-coating different concentrations of m-MTDATA on PTAA top layer.

m-M (mg/ml)	V_{OC} (V)	J_{SC} (mA/cm^2)	FF (%)	PCE (%)	Average PCE (%)
0	1.063	23.74	78.01	19.69	19.35±0.48
1	1.075	24.25	79.28	20.66	20.12±0.52
1.5	1.085	24.34	79.81	21.22	20.76±0.48
2	1.082	23.95	78.32	20.29	19.85±0.40
3	1.079	23.15	77.65	19.39	18.89±0.52

Table S5. Performance parameters of PSCs prepared by spin-coating different concentrations of PhABr on the Perovskite top layer.

PhABr (mg/ml)	V_{OC} (V)	J_{SC} (mA/cm^2)	FF (%)	PCE (%)	Average PCE (%)
0	1.063	23.74	78.01	19.69	19.35±0.48
0.75	1.085	23.90	79.28	20.66	19.87±0.39
1.5	1.098	24.29	78.97	21.08	20.82±0.27
3	1.102	22.62	78.27	19.52	19.13±0.40

Table S6. Performance parameters of PSCs prepared with the optimal concentrations in both top and bottom layers.

		V_{OC} (V)	J_{SC} (mA/cm^2)	FF (%)	PCE (%)
Pristine	Champin	1.063	23.74	78.01	19.69
	Average	1.056	23,23	77.56	19.03
Target	Champin	1.115	25.16	80.42	22.56
	Average	1.098	24.62	79.31	21.45

Table S7. Detailed R_s and R_{rec} values for electrochemical impedance measurements

PSCs with different treatment	R_s (Ω)	R_{rec} (Ω)
Pristine	14.13	1207
m-M	11.60	1488
Target	4.79	2285

Table S8. TRPL curve fitting parameters of Perovskite on original devices, PTAA/m-MTDATA devices, and dual-layer modified target devices.

Sample	A_1	$\tau_{1\ (ns)}$	A_2	$\tau_{2\ (ns)}$	$\tau_{ave\ (ns)}$
Pristine	328.81	93.79	175.85	1264.51	1121.92
m-M	438.44	73.03	245.18	806.12	703.91
Target	358.62	65.25	267.96	742.57	671.30

References

1. P. Hohenberg and W. Kohn, *Physical Review*, 1964, **136**, B864-B871.
2. W. Kohn and L. J. Sham, *Physical Review*, 1965, **140**, A1133-A1138.
3. G. Kresse and J. Furthmüller, *Physical review B*, 1996, **54**, 11169.
4. P. E. Blöchl, *Physical Review B*, 1994, **50**, 17953-17979.
5. J. P. Perdew, K. Burke and M. Ernzerhof, *Physical Review Letters*, 1996, **77**, 3865.
6. S. Grimme, J. Antony, S. Ehrlich and H. Krieg, *J Chem Phys*, 2010, **132**, 154104.
7. H. J. Monkhorst and J. D. Pack, *Physical Review B*, 1976, **13**, 5188-5192.